

N O T I C E

THIS DOCUMENT HAS BEEN REPRODUCED FROM
MICROFICHE. ALTHOUGH IT IS RECOGNIZED THAT
CERTAIN PORTIONS ARE ILLEGIBLE, IT IS BEING RELEASED
IN THE INTEREST OF MAKING AVAILABLE AS MUCH
INFORMATION AS POSSIBLE

"Made available under NASA sponsorship
in the interest of early and wide dis-
semination of Earth Resources Survey
Program information and without liability
for any use made thereof."

HEAT CAPACITY MAPPING MISSION (HCMM) PROGRAM

E82-10073

CR-165095

INVESTIGATION HCMM - Ø50

(E82-10073) HEAT CAPACITY MAPPING MISSION
(HCMM) PROGRAM: STUDY OF GEOLOGICAL
STRUCTURE OF SICILY AND OTHER ITALIAN AREAS
Final Report (Consiglio Nazionale delle
Ricerche, Milan) 34 p HC A03/MF A01

N82-20596
Unclassified
G3/43 00073

STUDY OF GEOLOGICAL STRUCTURE OF SICILY AND OTHER ITALIAN AREAS

P.I. Roberto Cassinis, Istituto per la Geofisica della Litosfera
Consiglio Nazionale delle Ricerche - Milano (Italy)

Final report
August 1981

Original photography may be purchased from
ERSOS Data Center

Sioux Falls, SD. 57198

Prepared by:

Roberto Cassinis, P.I.
Giovanni Lechi, Co-investigator
Eugenio Zilioli, Geology
Alberto Marini, Geology
Pietro A. Brivio, Physics
Nicola Tosi, Simulation model

RECEIVED

AUG 28 1981

SIS/902.6

HCMI - 050
Type III - Final

I - INTRODUCTION

The original objectives of the investigation included, as specified in the attachment A of the provisions:

- the study of geological structure of Sicily and the analysis of anomalous thermal areas
- the analysis of coastal waters around Sicily and NW Adriatic Sea.

During the course of the investigation, in order to have more chances to receive useful and complete data to fulfill the experimental goals of the investigation, it was decided by mutual agreement between NASA and the F.I. to extend the test area to other parts of the Italian territory; the primary goal of the experiment being to ascertain the potential of thermal inertia mapping as additional tool to discriminate the geolithological units.

The first complete day-night pass usable to compute the Apparent Thermal Inertia (A.T.I.) on one of the selected test sites (Sardinia) has been received only at the end of November 1979 (see 2nd progress report). For this reason, up to that date, we used incomplete data to test the equipment and part of the software.

In particular, we received one tape (A.A. HHP 783060111 - Scene identification A003801500) referring to a night I.R. pass (3 June, 1978).

The scene is centered on the Tyrrhenian sea (coordinates of central point N. $41^{\circ}46'11''$ - E $07^{\circ}56'23''$).

While the two original test areas (Sicily and NW Adriatic Sea) are out of the scene, the island of Sardinia appears not too cloudy and its image is of particularly good quality (Fig. 1).

On the other hand, Sardinia can be considered an excellent alternative target for the experiment. Its structural geology is well known and several geolithological units are distinguishable. The vegetation cover is generally very poor, in particular in June, on some of the outcropping formations (see paragraph III). Moreover, some of the rocks outcropping (granites, basalts, porphyries) are not easily found in other parts of the Italian territory; they appear as materials well suitable for thermal remote sensing because the relatively thin and uniform alteration coating.

Therefore, we decided to use Sardinia as a first training test area. The two CCT'S, received at the end of November 1979 (ident. numbers AA00590I4I03-AA0059I23702-AA0059I23701) contained the recording of the complete pass of June 24, 1978 (visible + night/day I.R.). These tapes are the only material so far received that can allow the computation of A.T.I., i.e., the main objective of the survey.

By a careful study of the image a test sub-area has been defined along the gulf of Orosei (Eastern coast of Sardinia). Here homogeneous night-day meteo conditions have been found together with a suitable geo-morphological and vegetational background.

II - TECHNIQUES

II.1 - Employed computers

For the analysis of the first digital HCMM data we used two different computing systems:

- a) IBM 370/I38 with 700 K byte memory, disks, tape units, line printer, for the development of the algorithms.
- b) PDP 11 Ø3 with 20 kwords memory, disks, tape unit, TTY, color monitor, three refresh memories for the display of the results in a fast, visible way.

The software of this computer, originally designed for Landsat tapes, has been modified and improved for the HCMM tapes.

II.2 - Radiometric calibration

Regarding the measurements of radiant power and the atmospheric corrections, so far we didn't apply any modification to the data.

No absolute measurements are foreseen, the survey taking into account only relative quantities.

II. 3 - Data handling and software

Our analysis of the available data from HCMM mission of the Explorer-A satellite has suggested to us to produce a suitable software in order to

accomplish the mission objectives. We preferred to write our own software instead of trying to adapt the software supplied by NASA. The software production concerned the following items:

- A) modification of the existing programs (mini-computer PDP 11 Ø3) in order to read the HCMM tapes (completed)
- B) realization of a software package which allows the comparison of images produced by different sensors and/or gathered on different orbits. In order to solve the registration problems we have written some algorithm to correct rotations, translations, deformations and to minimize the residual differences (completed)
- C) development of new programs to calculate temperature values from data indexes, to determine thermal inertia by day-night passes comparison.
- D) differential analysis by means of mathematical operators to study the spatial and temporal evolution of surface thermal parameters(completed)
- E) merging of the data contained on the HCMM tapes with other data (Land-sat, topographical and geophysical).
- F) An algorithm was written to represent on the slave monitor the profiles to be analysed; it is also possible to represent and print all the values of the pixels along the profiles.

II.4 - A.T.I. evaluation

The scene covered by the June 24 complete pass is illustrated in Fig. 2 (quick looks of visible and night/day I.R.).

The application of the algorithm suggested by NASA for the computation of A.T.I. gives the results illustrated by the image shown in figure 3a. Thermal inertia over land has been represented by nine levels (fig. 3b). In order to minimize the effect of the errors of registration a resampling program has been designed. Each original pixel was subdivided into nine "subpixels" whose values depend on the surrounding pixels: a second order function was studied in order to reach the best fitting with the original distribution. In such a manner we obtained a new set of images where the "geometrical resolution" is actually improved.

The image shows a very good definition both in geometrical and in A.T.I. function resolution.

III - ACCOMPLISHMENTS

III.1 - Description of selected test areas: the island of Sardinia (training test area)

The Island of Sardinia seems to exhibit peculiar characteristics, that cannot be easily found in adjacent areas.

Geography: the cloud cover is one of the lowest in the area due to the position of the Island, in the central part of the western Mediterranean Sea.

Furthermore, the coast line represents a good geographic reference and the surrounding sea is a natural source for the thermal calibration of images.

Orography is not exceedingly rough but a clearly differentiated morphology exists.

The wooden areas are confined to some well defined sites. Moreover, in the warm season, the vegetation influence is very low, owing to the dryness of the region.

Geology-Lithostratigraphy: a complete chronostratigraphic sequence is found, from the Cambrian to the present period. The outcrops are clearly definable; the morphology is typically shaped by plateaux in different aged limestones (Cambrian, Giurassic and Cretaceous, Eocene and Miocene). In the North-Eastern part of Sardinia a Hercynian batholith outcrops, as well as somewhere else in the southern area.

Geo-Tectonic framework: structural features of the area are not influenced and troubled by recent plications and folding. In general, the tectonic assessment shows a stretching fault style (graben of Campidano and normal faults and wrenches).

Geomorphology: the region shows different areas with peculiar aspects and characteristics:

- alluvial belt (NW-SE) corresponding to the rift valley of Campidano (South of the island)
- Permo-triassic peneplain with the subsequent mesozoic transgression which presently occurs under the form of isolated tableaux (Central-Eastern part of the Island)

- Plateau basalt with wide lavaflows to be related to the recent volcanic activity (Pliocene-Quaternary),

Other kind of data: we have the opportunity of correlating the results of the investigation with other available kind of data and information from space platforms and aircrafts;

- Skylab imagery
- Landsat passes
- Local thermal infrared aerial surveys
- Pancromatic aerial photography of the whole territory, in different scales and already interpreted
- Aeromagnetic maps (both detailed and regional).

III.2 - Description of the sub-test area (Gulf of Orosei, East Sardinia)

On the first complete day-night available pass of HCMM, a cloud-free sub area has been selected, where the geological features and the environmental situation seemed favourable for the experimental survey.

The sub area is located on the eastern part of the island, along the Gulf of Orosei. Different geolithological units and types of morphology are present. Considering the main topic of the investigation, i.e. rock-type discrimination, a rough estimation of thermal radiance, topography, vegetation cover ($^{\circ}$) and elevation has been done in order to eliminate the main sources of noise.

This correlation has been done along three significant geologic cross-sections in the window, AA', BB', CC' (figs. 4, 6 and 8).

The profiles are justified by the need of comparing different topographic and geologic trends. As far as the morphology is concerned two extremes can be considered along the coastal line: the steep calcareous cliffs and the flat alluvial lowlands (fig. 5).

($^{\circ}$) (using Landsat imagery - see 1st progress report)

The geological setting of the area concerns mesozoic and paleozoic sedimentary units submitted to low folding and modeled by a compressional system of reverse faults. Hercynian granites, perphyries and basalts outcrop somewhere, cutting the sedimentary formations in different ages.

III. 3 - Aerial distribution of A.T.I.

The image of fig. 3 shows the areal distribution of A.T.I. as displayed on the monitor of the computer system.

The results are displayed in 6 bit way using the refresh memory planes (64 gray levels) while the computations are developed in 8 bit way; therefore, there is a sort of data compression on the display.

For this reason the B & W image doesn't represent the whole information content, the 256 levels having been assembled into groups of 4; furthermore, the image contains only 72 levels, which have been compressed into 18 steps.

III. 4 - T.I.R. and thermal inertia profiles.

The first attempt of evaluation has been made comparing the geological cross-section, the topography, the I.R. radiance and the thermal inertia along selected profiles.

The night thermal radiance profiles do not seem to be always in agreement with the relief, except in Scala Manna Mnt. surroundings (see Sect. A-A' of fig. 6 and in low lands along the coast). The general trend of the thermal profile along the two sections A-A' and B-B' shows some correlations that could be summarized as follows:

- eruptive rocks (either extrusive and igneous) seems to have relatively higher radiance values.
Porphyrites, in particular, are well contrasting where a flat morphology occurs.
- Shales and associated rocks appear to be causing the decreasing of the values. This fact is well clear when porphyrites extrusions are closer to the shales.

- Generally, mesozoic carbonatic formations, as well as the alluvial sands and gravels, mantain lower values.

These considerations also apply in the vicinity of Scala Manna Mnt.
(see A-A').

- A negative spike (see section B-B') corresponds to the contact between giurassic and cretaceous dolomitic limestones.
- Positive spikes seem, in general, to mark the boundaries of the outcropping formations.

Thermal inertia profiles appear smoothed in comparison with the thermal radiance, as expected.

Given the large differences between water and land, we have introduced (A-A') two different scales. Giving a quick look at the A.T.I. profiles, few notes can be drawn:

- Sea-water maintain the largest values, as expected
- Brackish waters (for ex. the Tortoli pool)are well identified, in contrast with the surrounding alluvial deposits.
- Differences seem to be maintained between dolomites (higher A.T.I.) and limestones (lower) especially where a contact exists.
- A.T.I. peaks appear within granites outcrop, eastward of Isalle Creek (see Sect. A-A') as well as in Section B-B' (the latter of lower amplitude), perhaps corresponding to concentration of Silica (see III-5).
- A general decrease of A.T.I. although not everywhere confirmed, seems to correspond to eruptive rocks.

In general lithological contacts seem to have larger influence on A.T.I. than proper faulting in homogeneous formations.

In order to confirm these first encouraging results we established a new profile in the northern part of the same window where a more detailed field geology had been already carried out (fig. 7).

The section intersects three main lithologic units: calcareous mesozoic formations, basalts and granites.

In the geological map of Fig. 7, we can observe how the trace of the C-C' section is nearly perpendicular to the general NE-SW trend of the structural features, so that no appreciable variation would be met taking the measurements along parallel, closely located profiles,

Also the topography is represented by NE-SW valleys due to the reverse faulting in mesozoic limestones and hercynian granites,

Therefore three contiguous digital profiles were drawn instead of one only, where the central one (C-C') is along the middle section, while the other two are shifted (one pixel each) in opposite directions,

Furthermore, since the profiles are not perpendicular to the scan lines, a small shift (206 m.) occurs between the contiguous profiles to be compared. The location of these profiles is justified by the fact that in the area the vegetative cover is very poor, particularly at the time of the HCCM survey (June 24),

On comparing the geological profile C-C' with the night IR data we can deduce a general agreement with the topography, except than in the western part where a positive anomaly of radiance occurs along a slope (fig. 8a).

The three profiles of A.T.I. (fig. 8b) look very similar (the similarity is much higher than among T,I,R. profiles); their correlation with the geological features is much clearer, while almost no correlation is observed with the topographical profile,

The lowest A.T.I. is found on granitic and basaltic outcrops where their area is of sufficient extent (several pixels), while A.T.I. is higher on carbonatic and dolomitic or moist deposits. Almost every fault and contact is marked by a jump of A.T.I., the interval being sometimes of the order of one pixel.

This last remark seems to demonstrate the ability of A.T.I. to detect contacts or tectonically disturbed zones with a good resolution.

On the other hand it seems more difficult to measure the difference in A.T.I. between homogeneous materials having different lithology. However the areas of the exposures that we have surveyed are not sufficiently large to lead to a completely negative conclusion.

In the NW part of the profiles a regular positive trend is observed. The vegetation behaviour doesn't seem responsible for this increase, while it could indicate progressive change of the lithotype of granites. However, it is hard to exclude any influence of surface alteration and of difference in microfracture density.

III.5 - Ground surveys.

A ground survey has been accomplished along the profiles of fig. 6. The ground truth has been collected in order to try to explain the A.T.I. and thermal anomalies observed (fig. 9). The points where the relevant observations have been made and samples collected for further laboratory examination are marked with arrows and progressive numbers, namely:

- 1) the outcropping rock is a very acid pegmatitic granite.
The topography is flat and the vegetation is almost missing. Very thin soil cover, almost non-existent. Alteration sands are present in part of the area.
- 2) A morphological change (from flat areas to hills or typical plateaux) corresponds to the contact between granites and basalts.
- 3) The pattern illustrated in the sketch of fig. 9a could be accounted for the increase of the A.T.I.
- 4) The situation is illustrated in detail by the sketch "b" of the same figure. The anomaly can be originated by the strong contrast between the bare exposure of granites and the dolomites covered by high vegetation.
- 5) The observed area is located on a high plateau covered by an uniforme blanket of mediterranean vegetation. A small swamp area of $300 \times 200 \text{ m}^2$ and the presence of muck could influence the A.T.I. The granitic type is aplitic; therefore the alteration sands are much finer than at point 1 (ref. Fig. 9c).
- 6) The situation is here very clear. The vegetation reaches the highest density of Sardinia. A deep valley cut in limestones and covered by tall trees runs in NE-SW direction.

7) Geological cross section C-C' is characterized by two outflows of basalts, strictly related to the pliocenic disjunctive tectonics, and by the contacts between the mesozoic limestones and the granitic basement.

The topographic profile is connected to the lithological variations whose boundaries are enhanced by the erosion which has led basalts into a reversal of the relief configuration. General landscape can be assumed as a gently sloped morphology intersected by valleys deeply cut with steepened flanks of limestones. The situation of the basalt morphology contrasting the limestone walls has been already illustrated by the sketch "a" of fig. 9.

III.6 - A simulation model of diurnal temperatures of rocks having different thermal inertia.

An attempt has been done to evaluate the possibility of showing, by remote sensing measurement, the diurnal temperature variation on the surface of a rocky outcrop composed of different materials (6).

It is known that the difference between the daily maximum and minimum temperatures of a surface composed by a homogeneous rock is related to the thermal inertia of the rock itself.

This is rigorously true in the simplified hypothesis of neglecting other factors affecting the surface temperature, i.e.: the rock's moisture, the atmospheric humidity, the surface slope, the surface roughness, the wind velocity, the vegetal canopy, the thickness of the alteration cap, etc.

The thermal inertia (of solid) (P) is defined as:

$$P = \sqrt{\rho \cdot c \cdot \lambda} \quad (\text{cal/cm}^2 \cdot \text{k.s}^{1/2})$$

where ρ is the density of material, c the specific heat, λ the thermal conductivity.

From the above definition it comes out how different types of rocks, generally, exhibit different thermal inertia. The values for rocks range approximately between 0.02 (dry sandy soils) and 0.07 (solid rocks), the average for solid rocks being of about 0.04 c.g.s.u.

For this reason it can be sought that, measuring the soil temperature in two significant instants (one when the surface temperature is close to the maximum, the other when the temperature is close to the minimum, and determining the temperature excursion ΔT , useful information on thermal inertia of the rock can be extracted that can help in lithological discrimination.

In order to evaluate this possibility a mathematical model, that simulated the diurnal temperature variation of a rocky outcrop, is proposed. The numerical example of an island, composed of blocks of three different materials: dolomite, granite, clay (dry) is examined.

These three materials have been chosen for the simulation because they exhibit a rather different thermal inertia, in order to have relevant temperature differences between the three homogeneous blocks of the island. The block's surface is assumed to be bare, (i.e. without vegetation cover), solid and dry, the surrounding sea having constant diurnal temperature (i.e. the apparent thermal inertia of the water body is supposed to be infinite).

The island (fig. 11) is composed of three homogeneous formations. In agreement with the finite difference method the island is divided in blocks of parallelepiped shape with horizontal dimensions of 20 m x 10 m, and thickness of 0,5 m (fig. 10).

The daily temperature in the blocks have been computed up to the depth of 6 m; below this depth the temperature can be supposed constant during the day.

In the hypothesis that the island is situated at a latitude of about 40° North, and during springtime, the surface temperature of every block ($12 \times 16 = 72$ blocks), in which the island's surface is divided, has been computed.

Since the simulation of temperature in unsteady state has been initiated with uniform soil temperature all over the island, it has been necessary a certain amount of time before reaching the dynamic steady state, when the surface temperature of a general block reaches the same value, periodically, within a period of 24 hours.

In the simulation, after reaching the periodical steady state, the lowest and highest daily temperature's values for each block have been computed.

We define:

$$\Delta T = T_{\text{maximum}} - T_{\text{minimum}}$$

the difference between the maximum and the minimum value of the surface temperature.

It appears (table I) that for the blocks consisting of the same material, the difference ΔT is very small, in the order of some thousandth parts of one Kelvin degree, while along the lines across the boundaries between different materials (table II) ΔT of the order of some degrees are found.

Namely, passing from dolomite to granite the difference in ΔT is of $1,2 \pm 1,3$ K, while between granite and clay the difference reaches 3,2 K. However, it has to be pointed out that the very low P of the dry clay is responsible for this large ΔT , that is a case very seldom found in practice.

If the actual conditions would have been taken into account (i.e. soil moisture, humidity in the atmosphere, evapotranspiration from the soil, etc.) and if we had solved the energy-balance equation on the soil surface, remarkably higher values of thermal inertia would be found for the three materials, and especially for the clay.

The simulation model seems to lead to the conclusion that the discrimination of homogeneous blocks is theoretically feasible only for materials having a thermal inertia contrast not below the $30 \pm 35\%$, this contrast corresponding to a temperature difference of the order of 1 ± 2 K, given the assumed geographical and seasonal conditions.

III . 7 - Comparison between simulated and observed A.T.I.

Price [1], Watson [2] and others have already discussed the factors influencing the remotely measured $T_{\text{max}} - T_{\text{min}}$ of a surface and the relationship between this difference and the thermal inertia P (related to the actual physical properties of the surface).

DOLOMITE (Profile 00)

T_{\min} (K)	294.549	294.562	294.562	294.562	294.562	294.549
T_{\max} (K)	301.275	301.288	301.288	301.288	301.288	301.275
ΔT (K)	6.726	6.727	6.726	6.726	6.726	6.726

GRANITE (Profile 0'0')

T_{\min} (K)	294.163	294.173	294.173	294.173	294.173	294.163
T_{\max} (K)	302.160	302.171	302.171	302.171	302.171	302.160
ΔT (K)	7.997	7.998	7.998	7.998	7.998	7.997

CLAY (Profile 0"0")

T_{\min} (K)	292.960	292.966	292.966	292.966	292.966	292.960
T_{\max} (K)	304.168	304.175	304.175	304.175	304.175	304.168
ΔT (K)	II.208	II.209	II.209	II.209	II.209	II.208

$$\Delta T = T_{\max} - T_{\min}$$

Table I - Simulation model; temperature and ΔT along profiles running parallel to the boundaries

	T_{\min} (K)	T_{\max} (K)	$\Delta T = T_{\max} - T_{\min}$ (K)
DOLOMITE	294.512	301.235	6.723
	294.562	301.288	6.726
	294.562	301.288	6.726
	294.562	301.289	6.727
GRANITE	294.172	302.171	7.999
	294.173	302.171	7.998
	294.173	302.171	7.998
	294.174	302.172	7.998
CLAY	292.965	304.174	II.209
	292.966	304.175	II.209
	292.966	304.175	II.209
	292.940	304.147	II.207

Table II - Simulation model temperatures and ΔT along a profile crossing the boundaries

The type and thickness of the coating of the rock surface is very critical.

A 10 cm thick dry sandy soil masks completely an underlying solid rock.

In this case, the observed A.T.I. would experience a consistent decrease (more than 30%). On the other hand, large variations must be expect when the surface temperature is affected by convection processes.

Evaporation depends also on soil moisture: if the coating consists of humid soil, the A.T.I. values are increased by an amount depending on the moisture content and on the mechanism of evaporation.

The difficulties involved in taking account of these factors are very large. and we did not endeavour, so far, to introduce them into the simulation model.

We simply compared the observed A.T.I. profile with the profile of P values consistent with the type of some of the outcropping rocks,

We derived the P figures from the table 8.I of [7].

Though it is well known that A.T.I. and P cannot be coincident, the comparison of their relative values can be significant.

We assumed as reference two values, $P_{\text{granites}} = 0,052$ and $P_{\text{dolomites}} = 0,075$, that are very close to the figures chosen for the same rocks in the simulation.

For common solid rocks P can be considered with good approximation as proportional to the inverse of ΔT .

In fig. I3 the geological types of the cross-section C-C' have been redrawn (fig. I3a).

Then the A.T.I. values observed along the three sections of fig. 8_b have been averaged into a common profile (T^*) and compared with the P values taken from [7] (I3c)

The third graph (I3d) represents the difference $b-c = A.T.I. - P$ assuming as reference the value $P = 0,052$ for granitic rocks.

It has to be noted that, in general, the A.T.I. profile is more irregular than the P profile. The second remark is that the areas where A.T.I. looks more constant (the "plateaux" in the curve) correspond to the largest outcrops of solid rocks (granites and basalts). A third remark is that the irregularities are found mainly among the high values of A.T.I.

The stronger irregularities of A.T.I. versus P can be explained either with the presence of a thin coating with lateral variations in thickness or composition, or with rock alterations or even with a variable moisture content.

It must be considered that the size of a riverbed (dry or moist) or of a depression filled with loose deposits (often related to faults or fracture zones) is generally smaller than one pixel. Therefore the narrow peaks or lows in the A.T.I. profile do not reach the amplitude corresponding to the actual A.T.I. but only indicate a trend (negative or positive).

The negative anomalies could be produced by dry soil, while the positive ones could be originated by moisture along drainage lines.

Nevertheless, by inspection of the residual profile of fig. I3 c we find that the A.T.I. and P profiles show a fair similarity, especially where bare, solid rocks outcrop.

They considerably diverge only in the NW portion of the profile, where, so far, an explanation cannot be found to account for the progressive increase of A.T.I. in granites.

IV - Significant results

The full potential of thermal inertia mapping as tool for rock discrimination has been only partially explored in this investigation. This is mainly due to the lack of repetition.

The repetitive, day/night passes over the same site can reduce the noise factors, as differences in atmospheric transparency, solar heating of the slopes , seasonal effects on moisture, vegetation etc.

However, the analysis of one single complete pass can lead to some relevant conclusion making a detailed comparison of A.T.I. profiles (or groups of parallel profiles) with T.I.R., geology and topography.

Namely:

- A.T.I. seems very sensitive to lithological boundaries and to tectonic disturbances. Alteration and moisture content seem mainly responsible for this behaviour of A.T.I.

- The difference between the A.T.I. average value of blocks of different lithology is, in general, small.

This behaviour is proved by the simulation model. However, provided that the blocks are composed of materials having a remarkable difference of P and a sufficient areal extent, the lithological discrimination seems feasible.

- On dry units of uniform lithology, with very little and uniform vegetation canopy, A.T.I. anomalies due to rock alteration can be observed. The block must have a size compatible to the resolution (at least 3 x 3 pixels).

The sub-pixel resampling technique is a useful approach to enhance this kind of effect.

The combination with Landsat imagery seems to be important in order to define the type and regularity of vegetation canopy.

- The simulation models of temperature transitory stress the need of repetition to minimize the effect of the different types of noise.

They also demonstrate the difficulty to discriminate rocks having A.T.I. differences less than 30±35%.

As far as the new data provided by HCMM, we can conclude that the acquisition of thermal inertia as well as of thermal radiance maps with the resolution of 600 x 600 m is an outstanding achievement; we feel that the results of the HCMM investigation will have a considerable influence on the future programs of Earth observation from Space.

Therefore we believe that new missions of satellite-borne thermal sensors, with suitable spatial and spectral resolution, should be planned considering the experience of HCMM.

We also believe that more conclusive results could be obtained by redistributing suitable data among groups of P.I.. This follow-on of the investigation could be prepared by specialized symposia organized through discipline leaders.

Reference:

- [1] - Price J.C. "Thermal inertia mapping. A new view of the earth".
Journ. Geophysical Research, vol. 82, N. 18, June 1977.
- [2] - Watson K.: "Periodic heating of a layer over a semi-infinite solid"
Journ. Geophysical Research, vol. 78, N. 26, Sept. 1973
- [3] - Rowan L.C. et al: "Thermal infrared investigations, Arbuckle
Mountains, Oklahoma", Geol. Soc. of Am. Bull. vol. 81,
Dec. 1970
- [4] - NASA HCMM users' guide, G.S.F.C., Dec. 1978
- [5] - HCMM investigation Ø5Ø. Progress reports:
August 1979
January 1980
October 1980
- [6] - Tosi N.: "A simulation model of heat flow and temperatures of rocks
having different thermal inertia". In press, Jan. 1981
- [7] - Barry S. Siegal, Alan R. Gillespie: "Remote Sensing in Geology".
John Wiley and Sons, New York, 1979

FIGURE CAPTIONS

Fig. 1 - Sardinia Island, as seen from HCMM pass-June 3, 1978 -
Night IR band. On the eastern coast the frame indicates
the sub test-area (Gulf of Orosei)

Fig. 2 - Quick looks of the available complete pass - June 24, 1978.
Reference: CCT AA0059I23701 - AA0059I23702 (a,b) day
visible and IR and CCT AA00590I4I03 (c) night IR.

Fig. 3 - Display of ATI by the application of NASA algorithm(a) -
and visualisation of a suitable contrast stretching opera-
ted on the same image (b). The black pixels indicated by
an arrow correspond to the highest values of ATI (gray scale
offset). See also the digital profiles of fig. 8.

Fig. 4 - Geologic map of the investigated window (Gulf of Orosei).

Formations:

γ = hercynian granites, β = pliocenic basalts,
 π = paleozoic porphyries, d = debris, q = quaternary alluvial deposits
gc = giurassic and cretaceous carbonates.
tg₁ = triassic and lower giurassic evaporites and carbonates
cs = silurian clayey shales; as = arenaceus shales (silurian - ordovician).

Fig. 5 - Topographic map of the investigated area.

Fig. 6 - Geology, night IR and ATI profiles along the cross sections
A-A' and B-B'

Fig. 7 - Detailed geologic map for the formations surrounding the C-C' section:

γ = hercynian granites, β = pliocenic basalts,
d = debris, q = quaternary alluvial deposits;
cr = cretaceous carbonates, g₂ = upper giurassic carbonates,
g₁ = lower giurassic limestones and dolomites

Fig. 8 - Geological C-C' cross section compared with contiguous digital profiles in the Night IR (a) and ATI (b) evaluation.

Fig. 9 - Geological sketches of the points indicated in fig. 6 along the traces of A-A' and B-B' sections

Fig.10 - Geometry of the model used for the simulation

Fig.11 - Subdivision of the "island" into horizontal plane blocks

Fig.12 - Daily temperature variations at the surface of the three blocks having different thermal inertia P.

Fig. I3 a) -Geological cross section C-C' (see fig. 8)

b) -A.T.I. profile (average of the three profiles C_1-C_1' , $C-C'$, C_2-C_2'). The scale on the right is the conventional one, the one on the left is a P scale transformed taking as reference the thermal inertia of granites (γ) and of dolomites (γ_2 , γ_1)

c) -P profile according to [7]

d) -Difference b-c = A.T.I. - P

ORIGINAL PAGE
BLACK AND WHITE PHOTOGRAPH

E 8°

N 41°

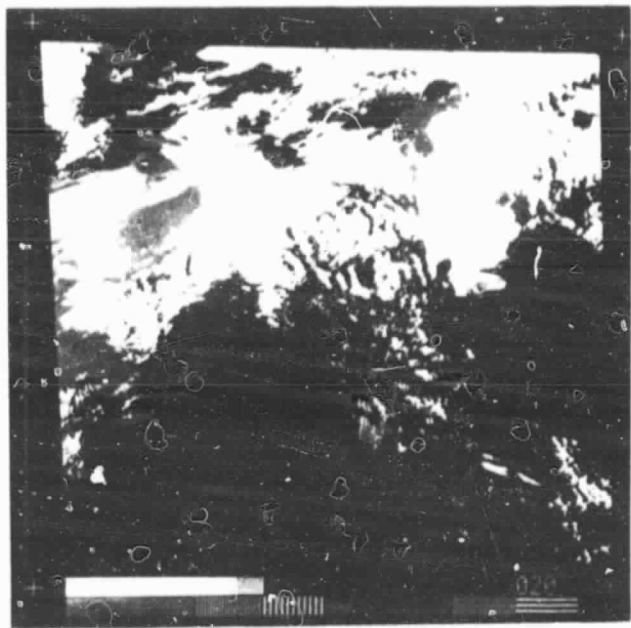
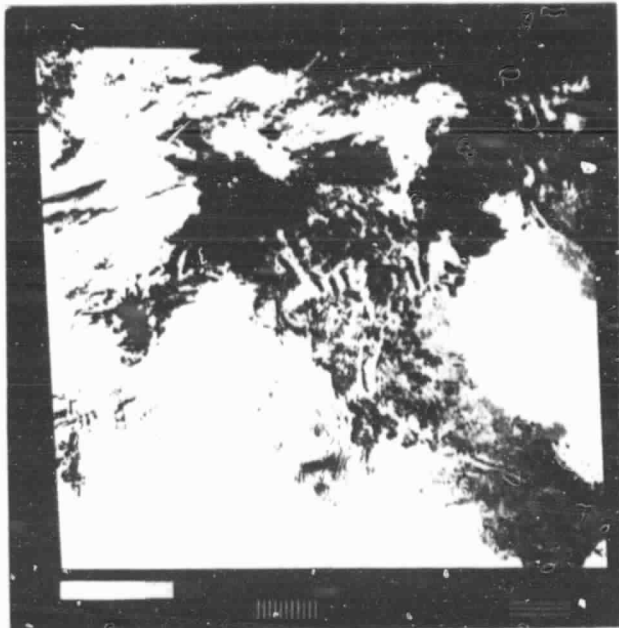
N 40°



0 10 40 km

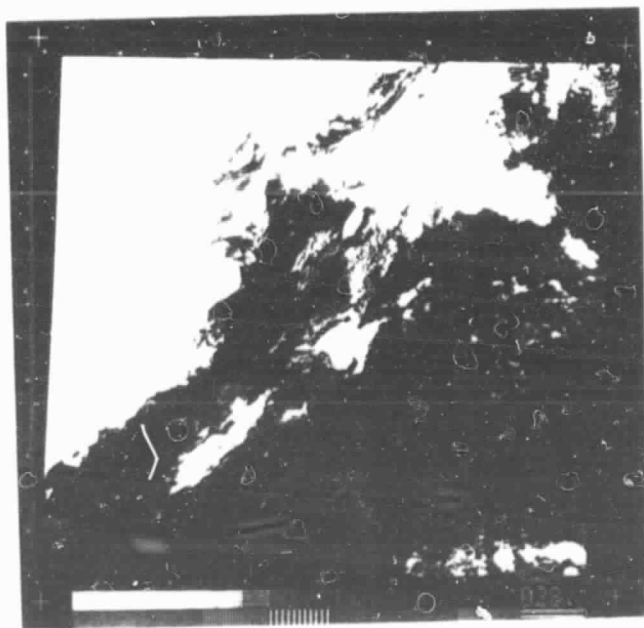
E 9°

N 39°



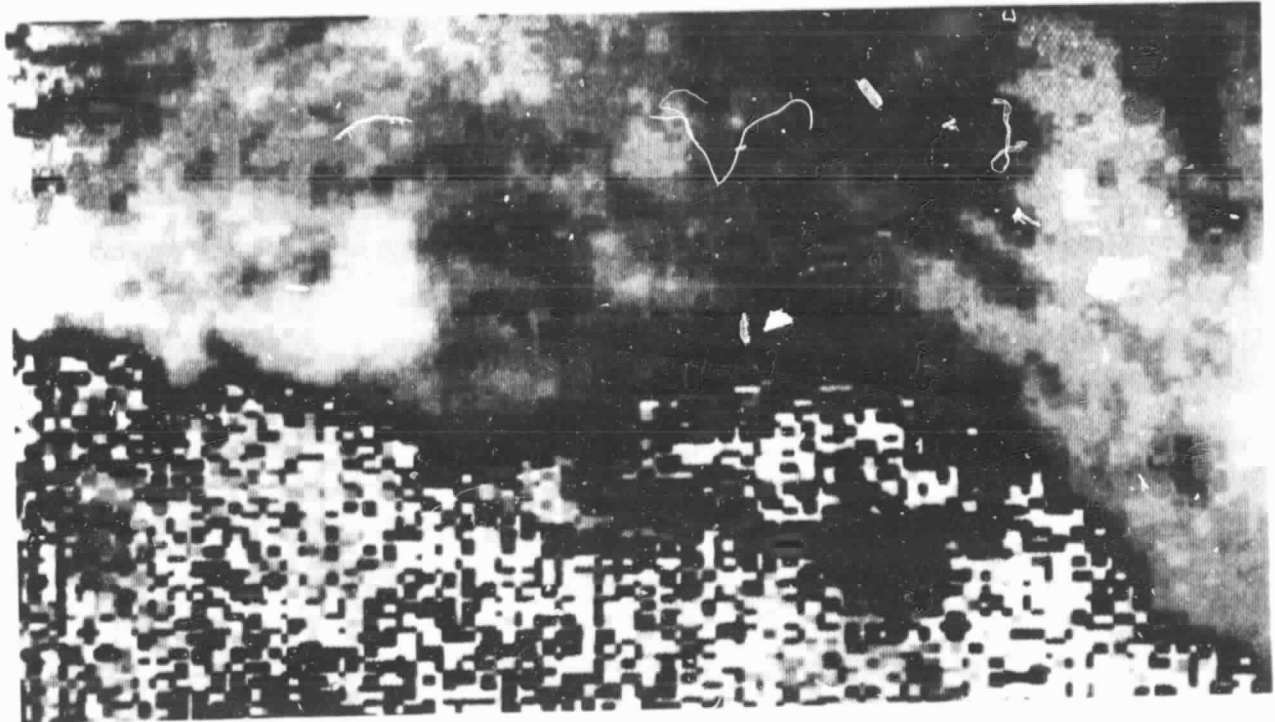
(a)

(b)



(c)

ORIGINAL PAGE
BLACK AND WHITE PHOTOGRAPH



(a)



(b)

ORIGINAL PAGE
BLACK AND WHITE PHOTOGRAPH

Fig. 3

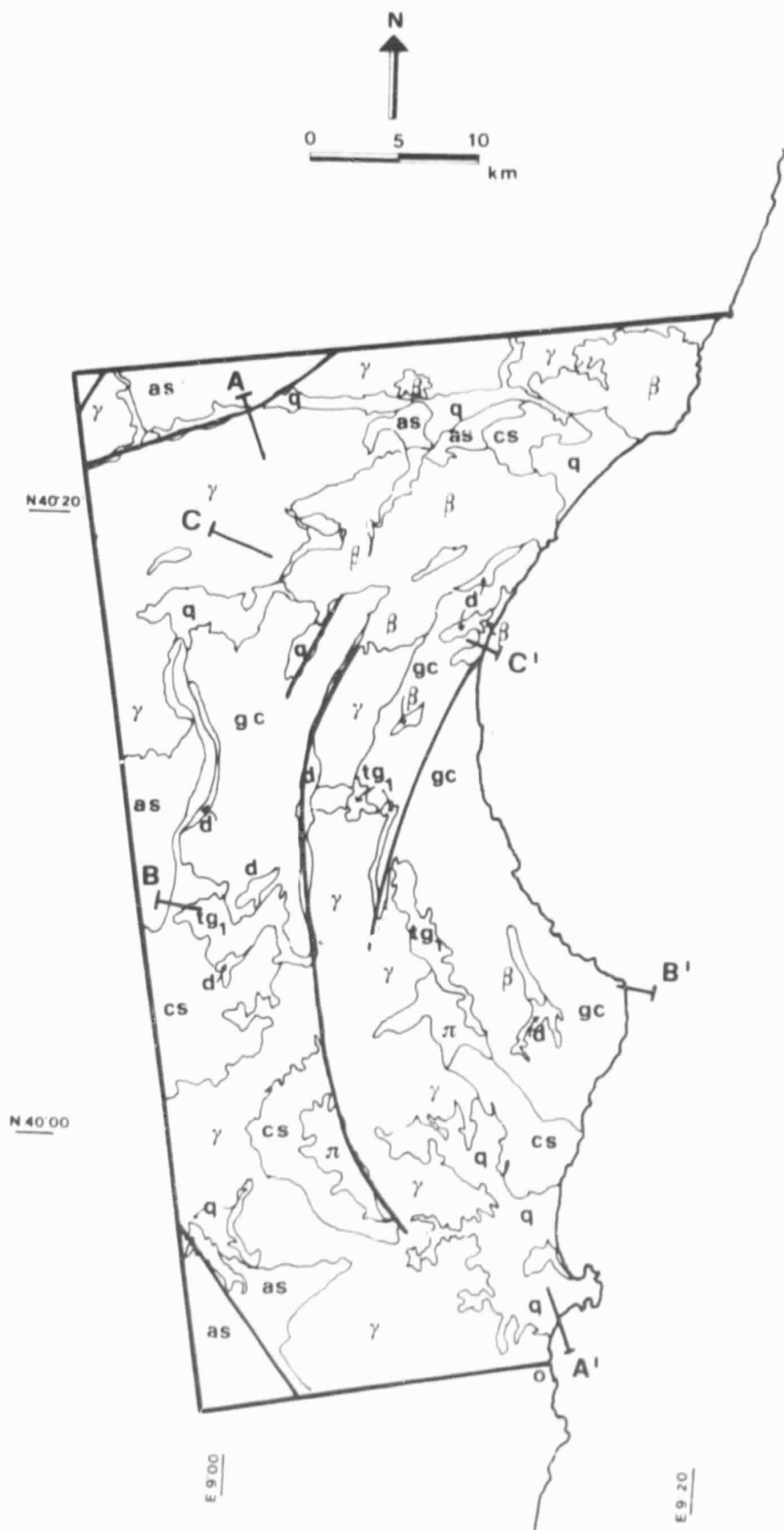


Fig. 4

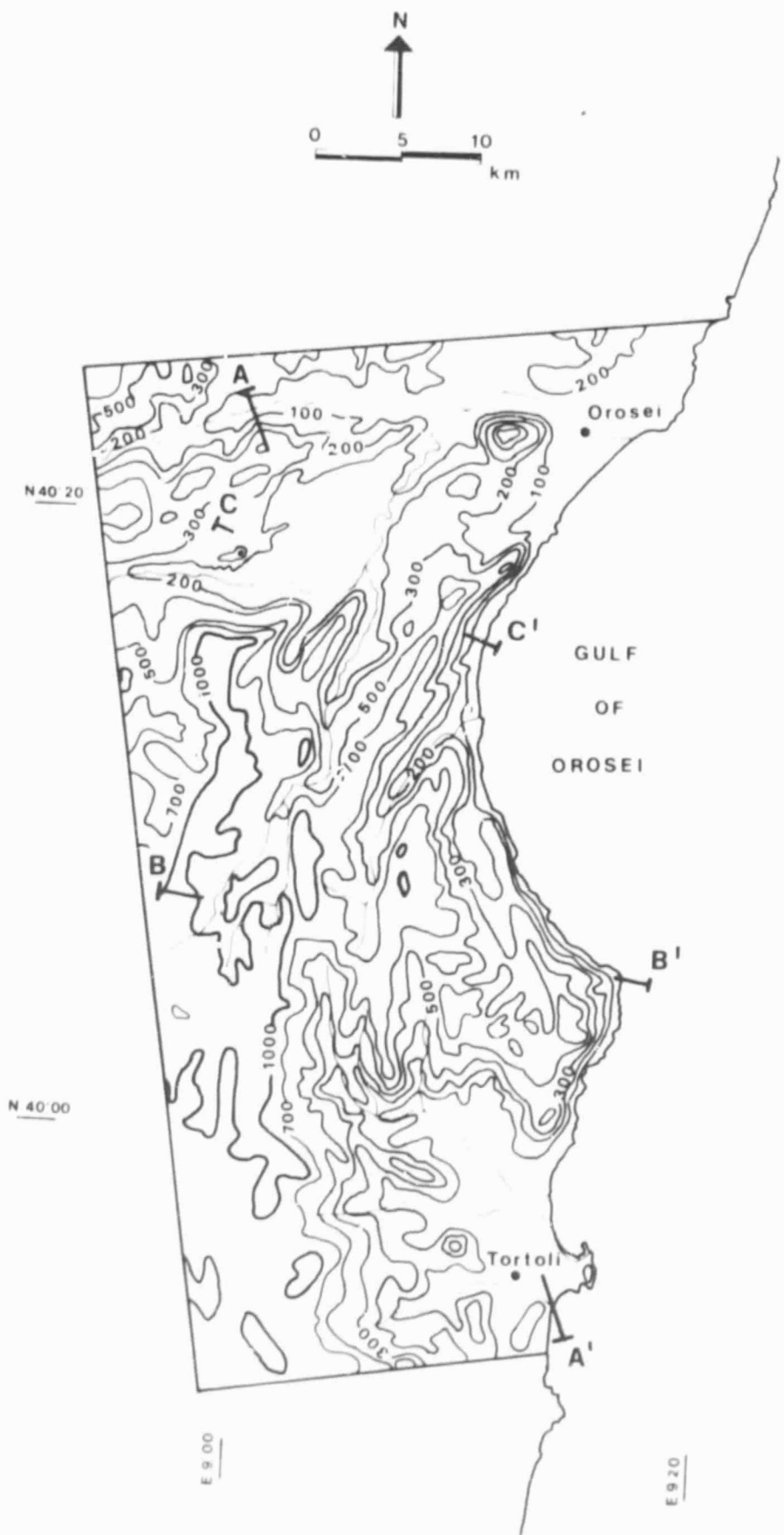
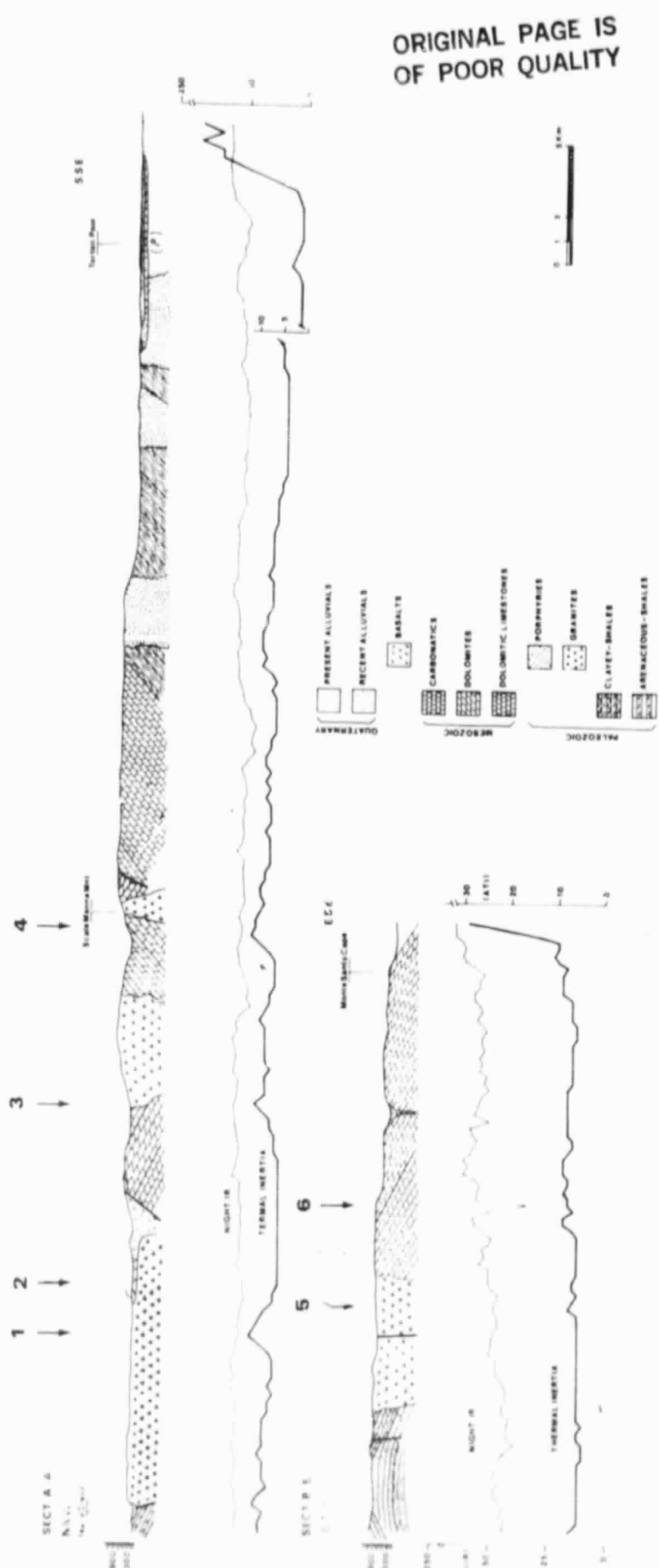


Fig. 5



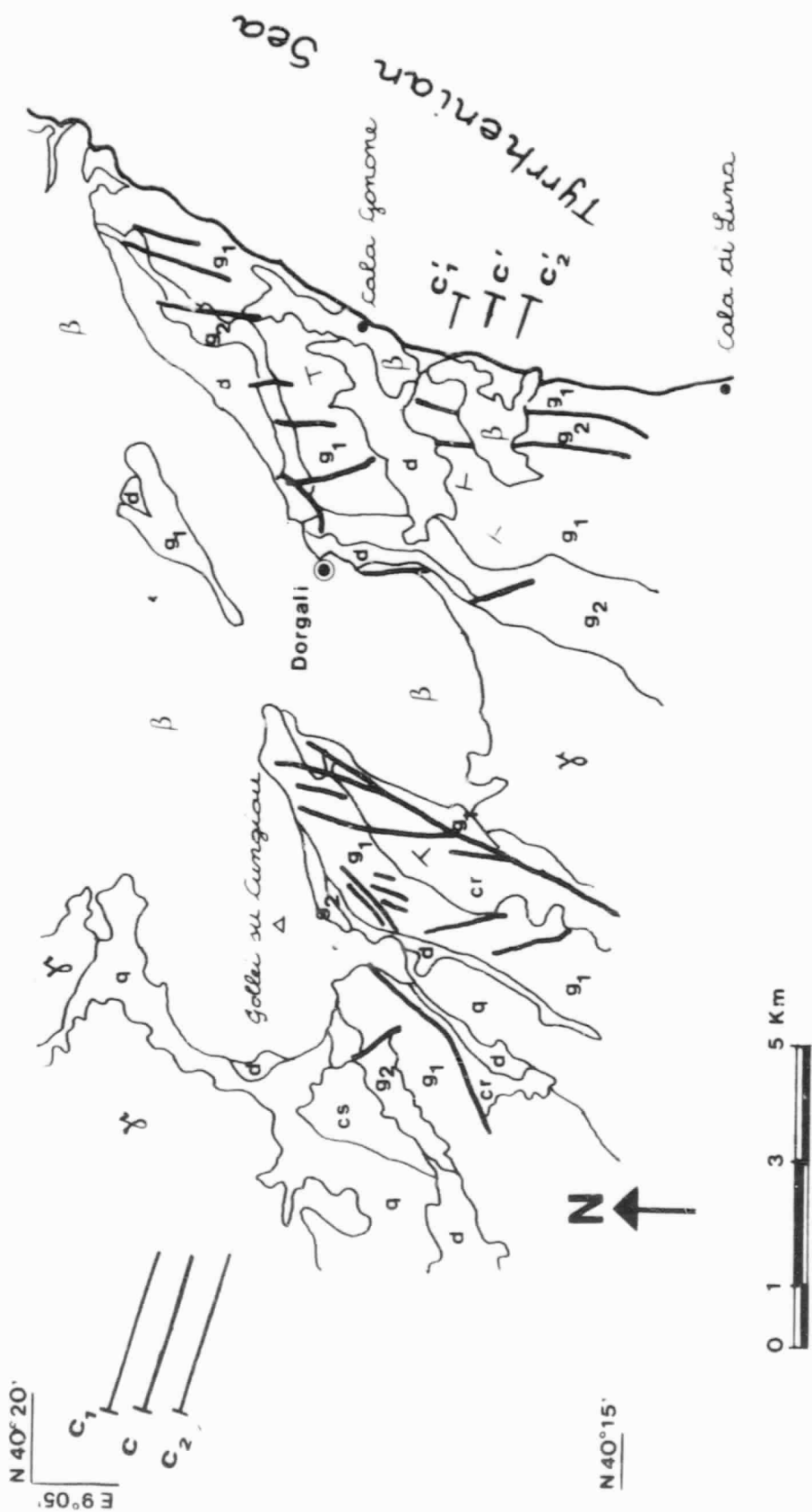


Fig. 7

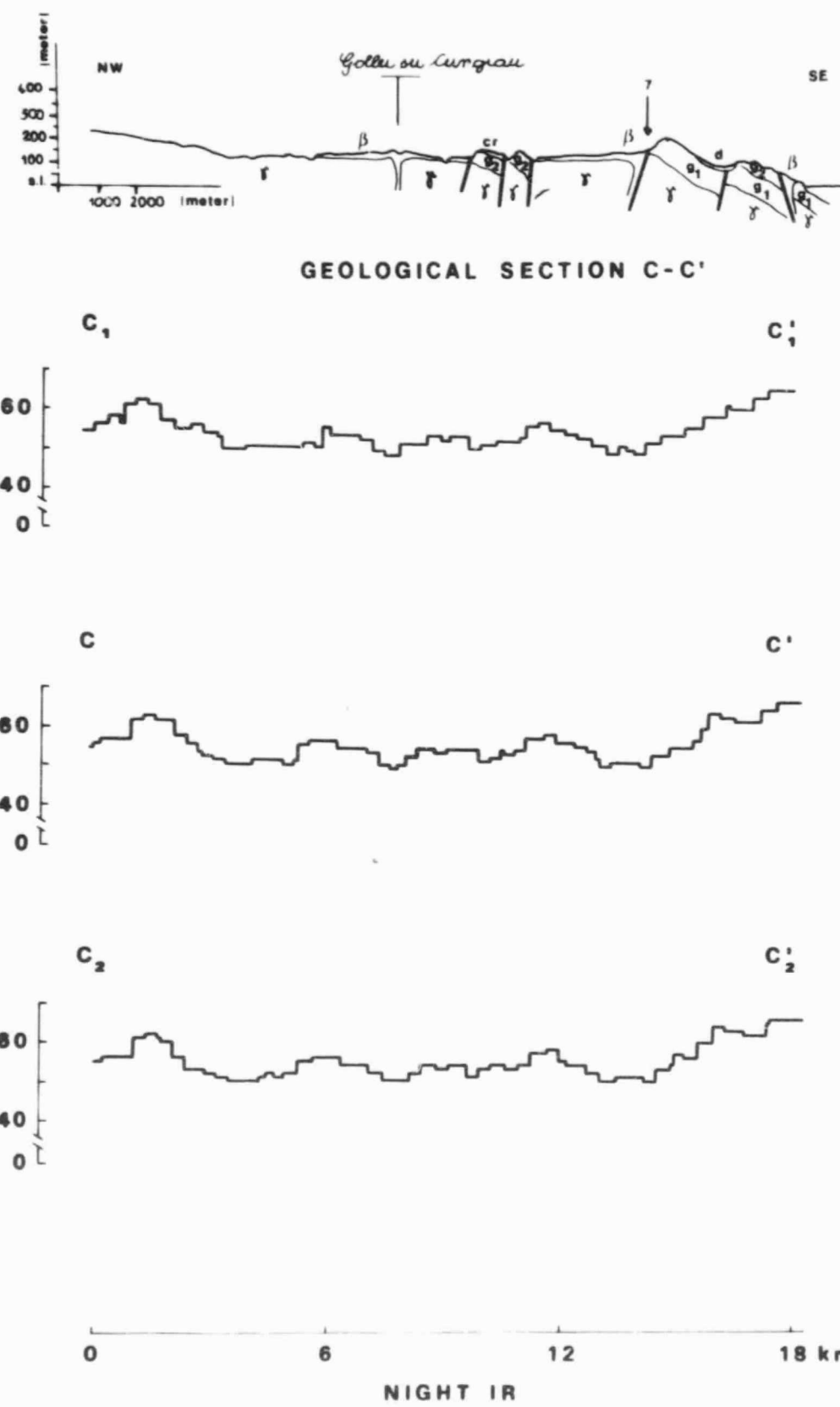


Fig. 8a



GEOLOGICAL SECTION C-C'

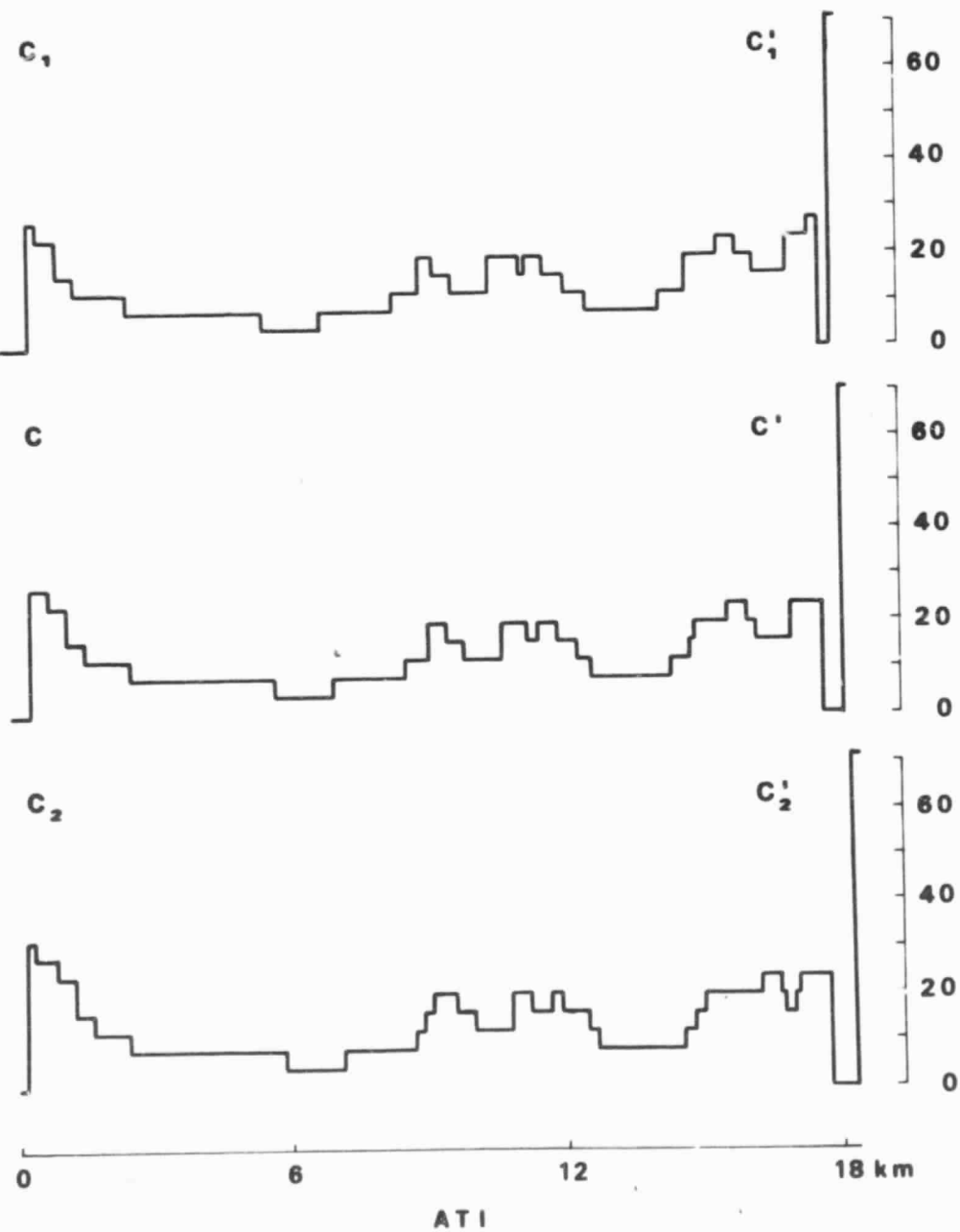
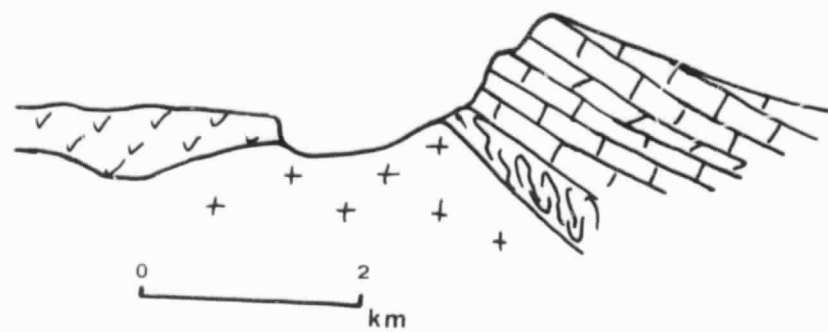


Fig. 8b

WSW

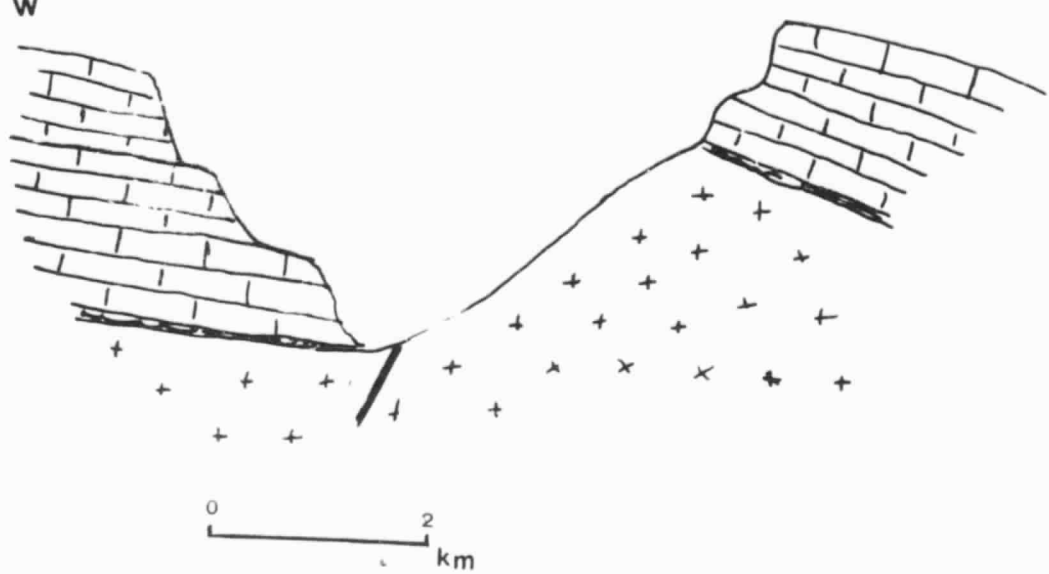
ENE



A

W

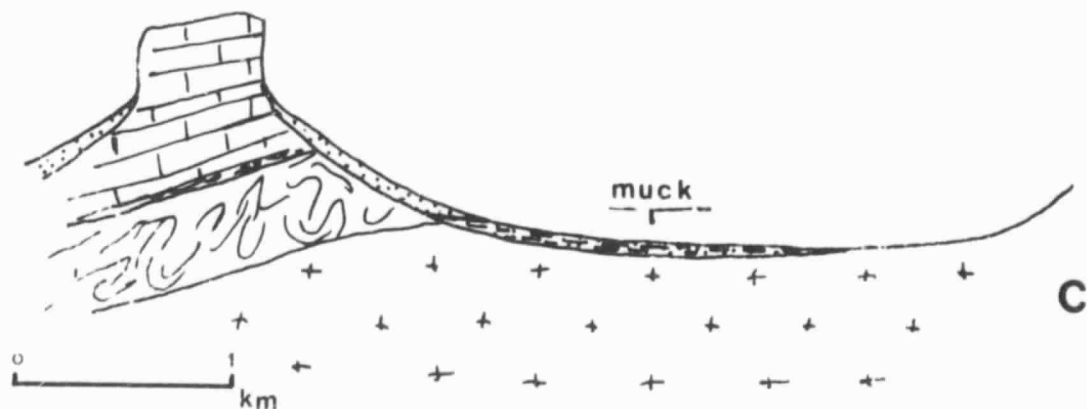
E



B

NW

SE



C

Fig. 9

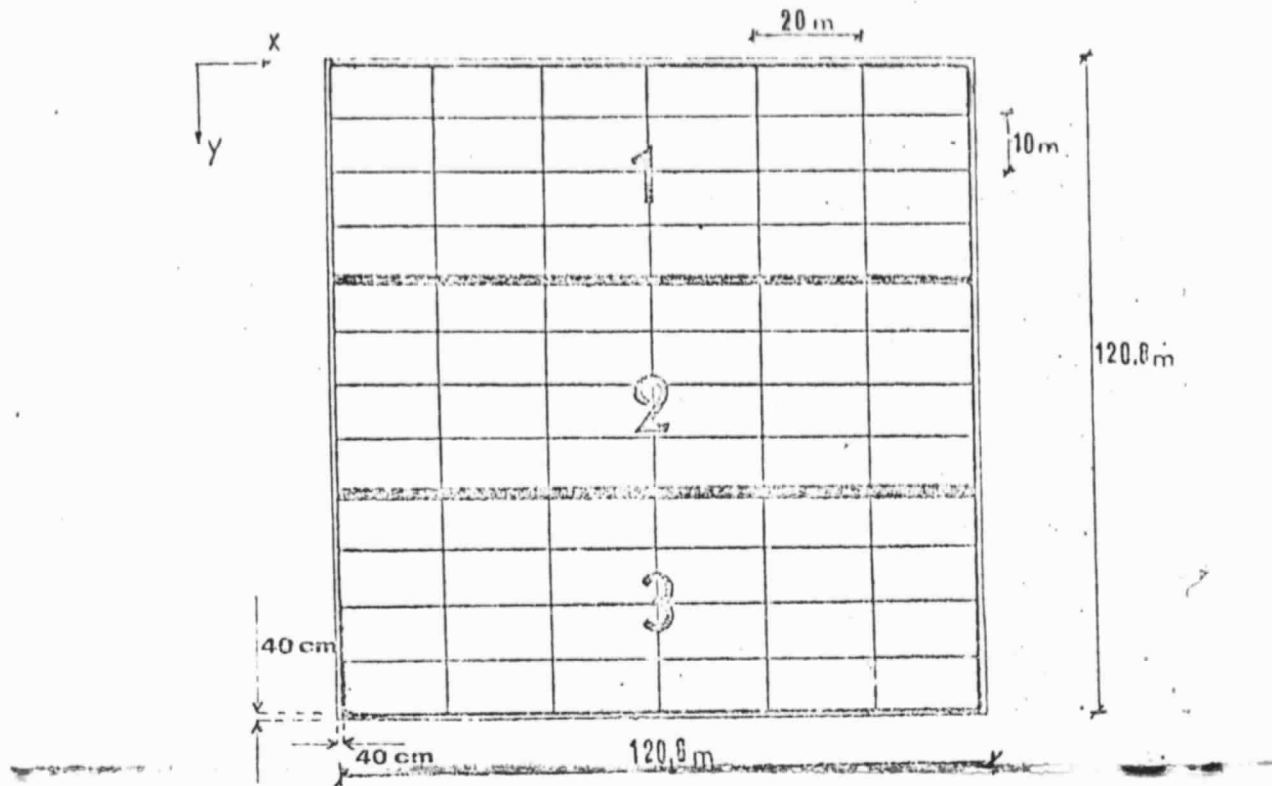


Fig. 10

ORIGINAL PAGE IS
OF POOR QUALITY

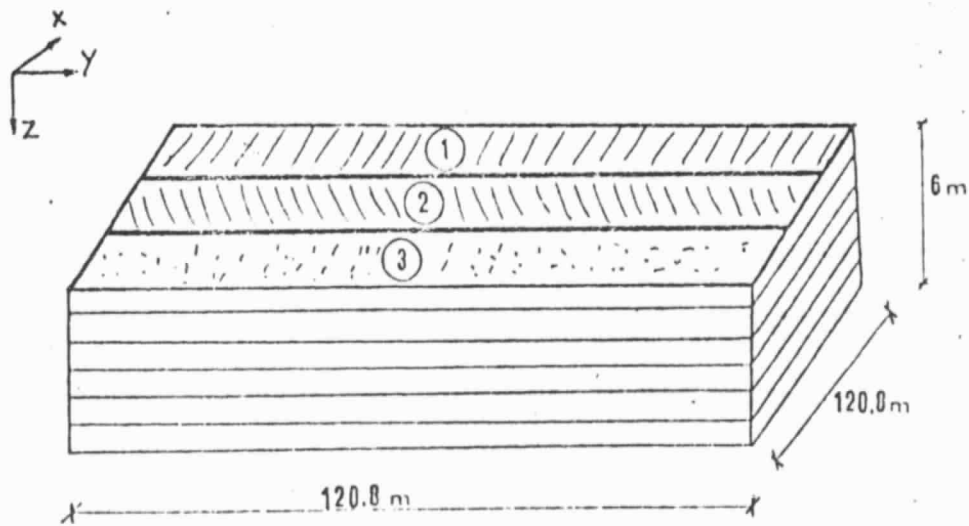


Fig. 11

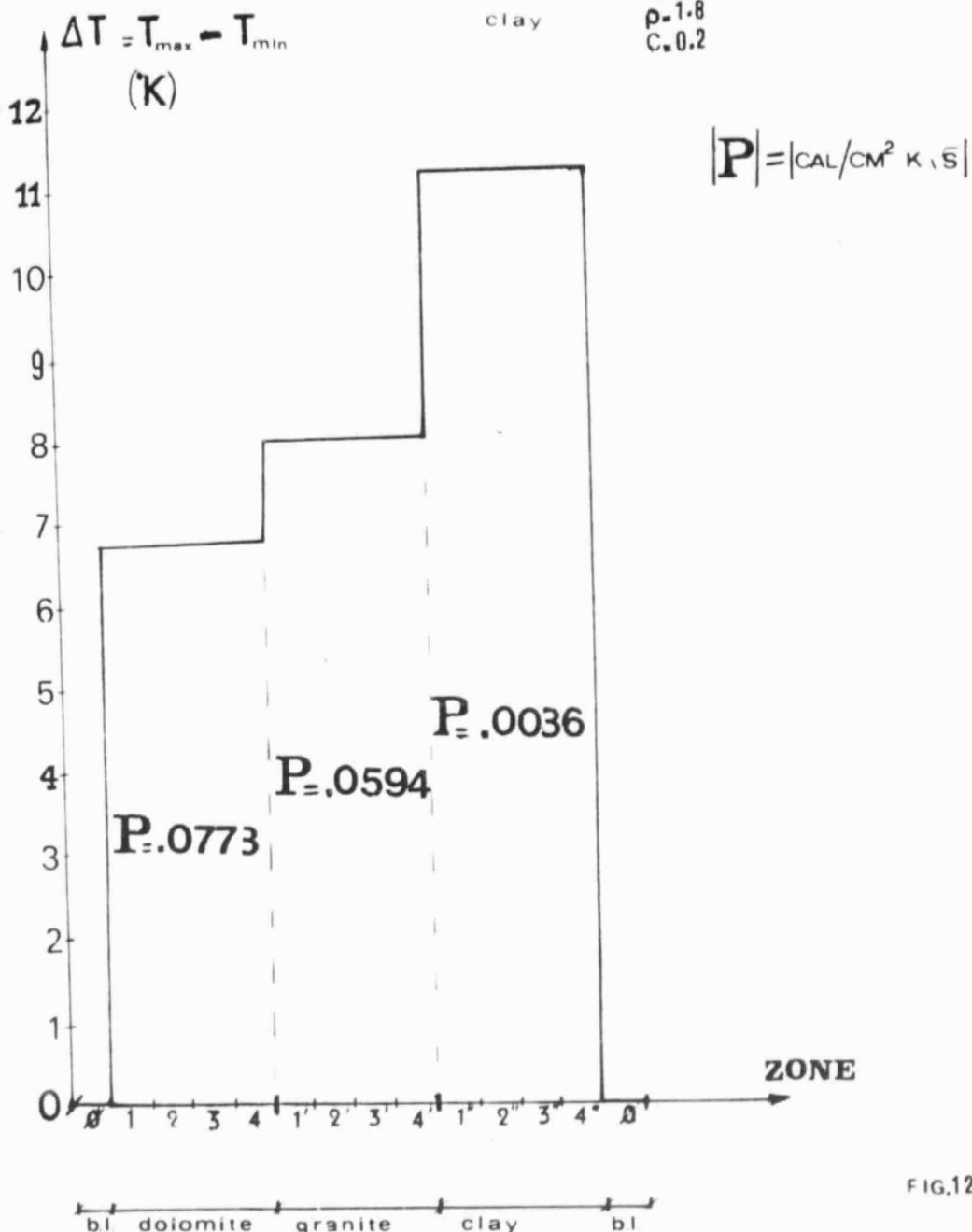
DAILY TEMPERATURE VARIATIONS

dolomite $\lambda = 0.01$ $\text{CAL}/\text{CM} \cdot \text{s} \cdot \text{K}$
 $\rho = 2.6$ g/cm^3
 $C = 0.23$ $\text{CAL}/\text{g} \cdot \text{K}$

granite $\lambda = 0.007$
 $\rho = 2.52$
 $C = 0.2$

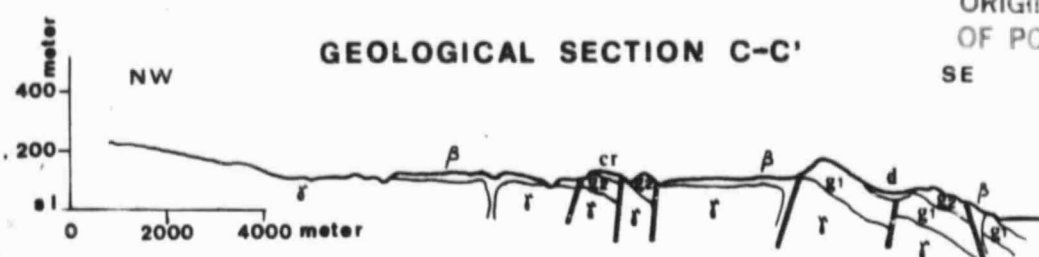
clay

$\lambda = 0.0036$
 $\rho = 1.8$
 $C = 0.2$



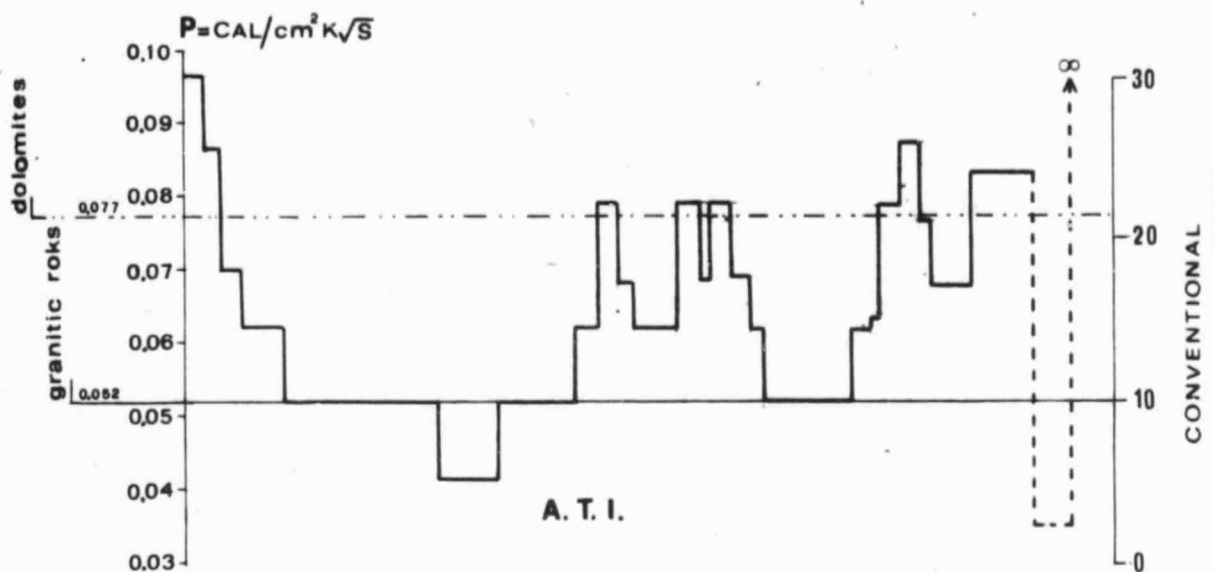
b.l.: border line

FIG.12

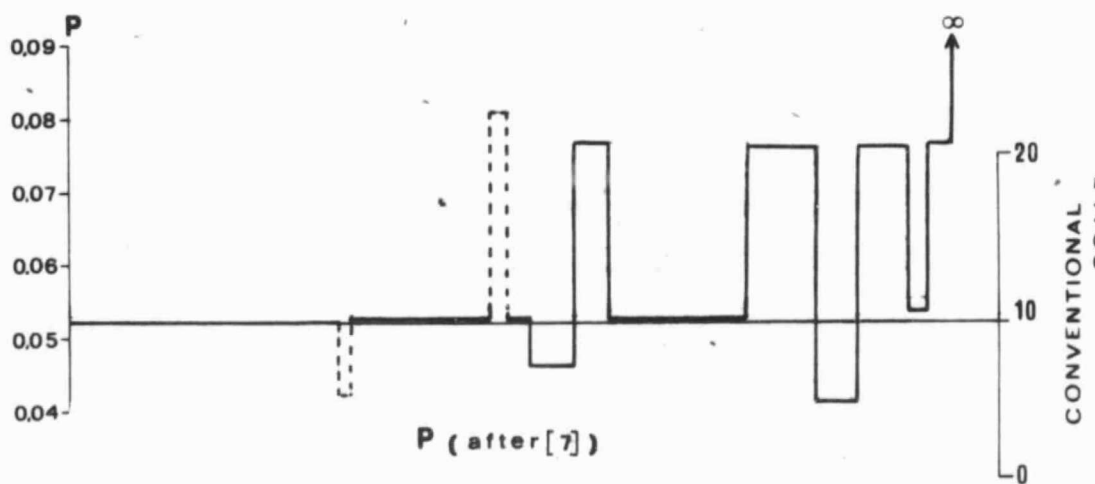


ORIGINAL PAGE IS
OF POOR QUALITY

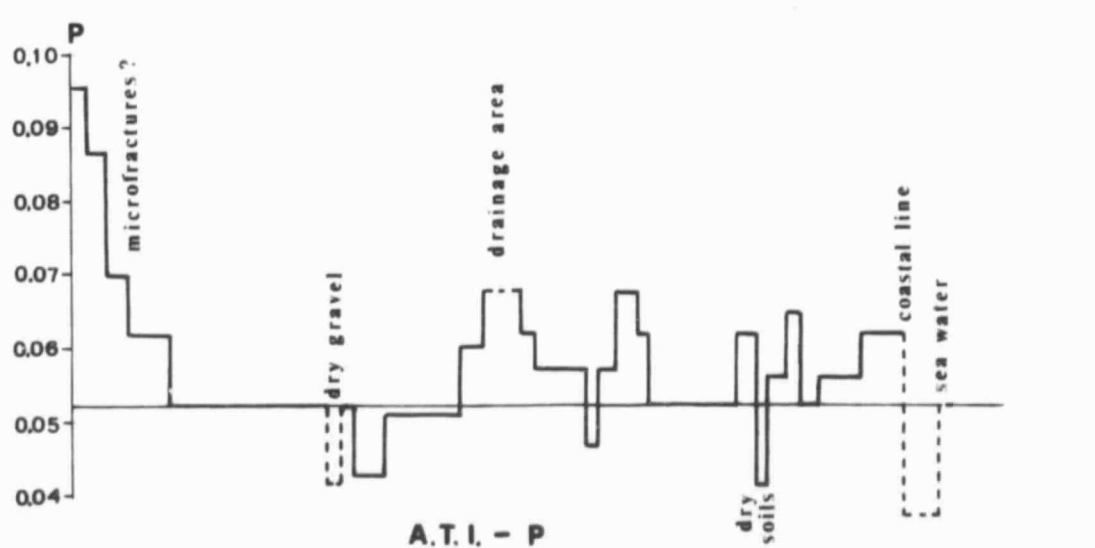
a)



b)



c)



d)